Biophysical Journal, Volume *111*

Supplemental Information

Costs of Clock-Environment Misalignment in Individual Cyanobacterial Cells

Guillaume Lambert, Justin Chew, and Michael J. Rust

Supporting Material for:

Costs of Clock-Environment Misalignment in Individual Cyanobacterial Cells

Guillaume Lambert[1], Justin Chew[2], and Michael J. Rust[1]

[1] Department of Molecular Genetics and Cell Biology, Institute for Genomics and Systems Biology, University of Chicago, 900 E 57th Street, Chicago, IL 60637, United States

[2] Medical Scientist Training Program, Pritzker School of Medicine, University of Chicago, 924 E 57th Street, Chicago, IL 60637, United States

Contact: mrust@uchicago.edu

SUPPLEMENTAL DATA

Supplementary Movie S1. Single-cell microscopy and mixed-phase experiments. Time-lapse move showing wild-type cells in multiple phases growing in the same field of view. Production of yellow fluorescent proteins is under the control of the PkaiBC clock-dependent promoter.

Supplementary Movie S2. Dormancy following prolonged darkness. Movie showing wild-type cells being subjected to an 18h pulse of darkness. White arrows indicate which cells entered a state of arrested growth.

Supplementary Movie S3. Response of Δ*kaiBC* mutants to 18h dark pulse. Movie showing a mixture of wild-type and Δ*kaiBC* cells being subjected to an 18h pulse of darkness. A larger fraction of Δ*kaiBC* cells display filamentous morphology compared to wild-type cells. Δ*kaiBC* cells at the beginning of the movie are called out with red arrows.

Supplementary Movie S4. Response of *kaiBC*-overexpression mutants to 18h dark pulse. Movie showing a mixture of wild-type and *kaiBC*-overexpression cells being subjected to an 18h pulse of darkness. *kaiBC*-overexpression cells display abnormal rounded morphology compared to wild-type cells. P_{trc} :: *kaiBC* cells at the beginning of the movie are called out with blue arrows.

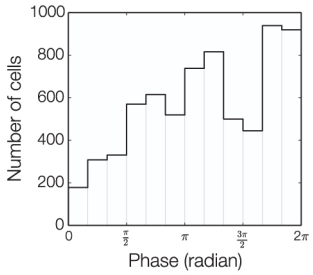

FIG. S1. Distribution of initial clock phases in single cells, estimated using the phase information from a Fourier transform of the EYFP reporter time series.

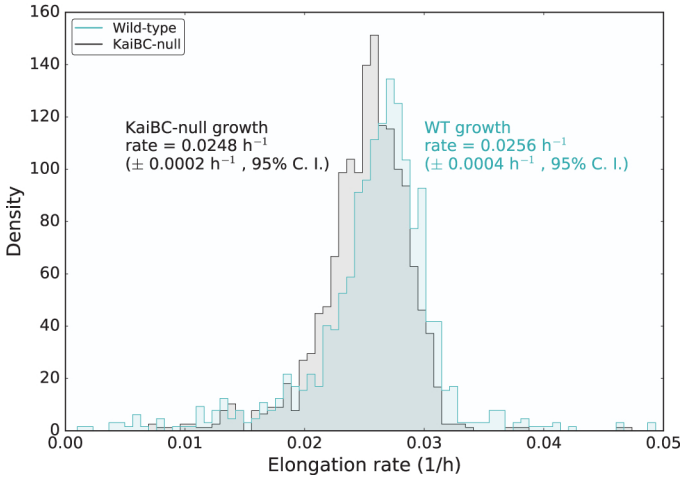

FIG. S2. Distribution of instantaneous growth rates of WT and Δ*kaiBC* cells grown side-by-side on the microscope. Each data point in the distribution is the average elongation rate for one cell over the microscopy time course (N=989 for WT and N=1189 for Δ*kaiBC*). Means are different at a $> 95\%$ confidence level.

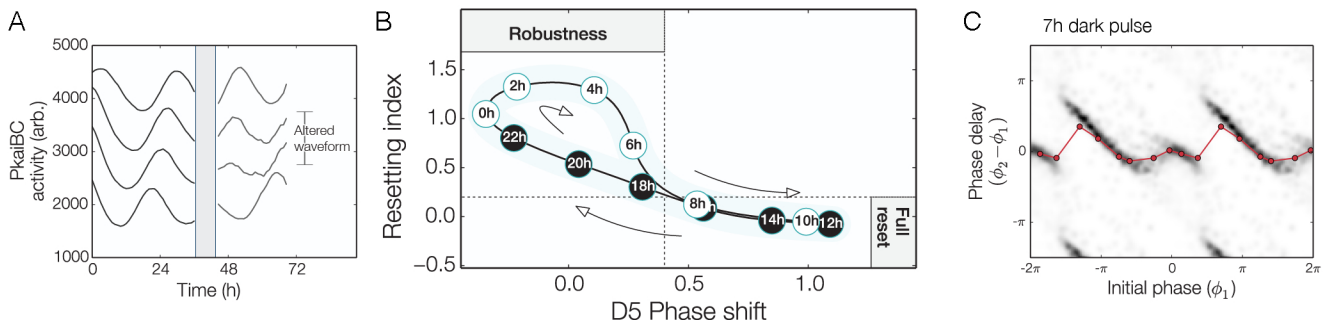

FIG. S3. Single cell phase resetting data A.) Averages of EYFP reporter signals before and after a dark pulse from groups of cells corresponding to approximately $3\pi/5$-wide bins of initial phase ($>$ 600 cells per waveform). B.) Model of the timekeeping switch between robustness and full clock reset. Robustness is defined as the magnitude of the phase shift following a 5h dark pulse. The resetting index measures the angle between subjective dusk (π) and the posterior phase ϕ_2 following a 9h dark pulse. Subjective circadian times are inscribed inside each datapoint. C.) Comparison between the single-cell density distribution of the phase delay following a 7h dark pulse, and a population average (red). Phase shift data for the average is binned under a 2h window.

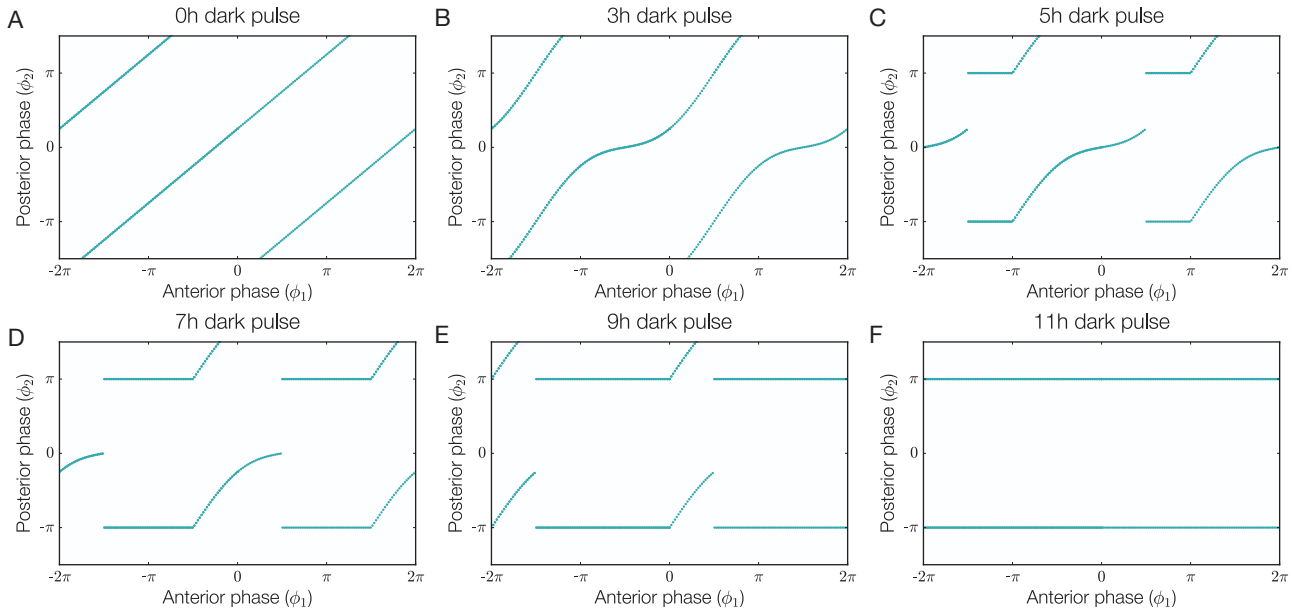

FIG. S4. Phenomenological model of clock resetting. Plots of the interpolating function:

$$f_n^P(\phi_i) = \begin{cases} \pi & \text{if } \frac{6\pi(n-9)}{P} < \phi_1 < \frac{\pi}{2} \text{ or } \phi_1 > \frac{6\pi(n-1)}{P} \\ \phi_i - \frac{6\pi(n-1)}{P} + A \cdot sin(\phi_i - \frac{6\pi(n-1)}{P}) & \text{otherwise} \end{cases}$$

for period $P = 24$h, and various values of the the dark pulse length n.

Peak time	Gene function	KEGG pathway
Dawn	Photosynthesis, chlorophyll production and carbon fixation	195, 860, 710
	Biosynthesis of amino acids	290, 400
	tRNA	970
	Steroid synthesis	100
	Fatty acids pathways	61
	Metabolism of amino sugars, amino acids, and purines	530, 330, 252, 280, 230
	Sugar metabolism, respiration, CoA biosynthesis	51, 130, 770
Dusk	Ribosome	3010
	RNA polymerase	3020
	DNA replication, homologous recombination and mismatch repair	3030, 3440, 3430
	Metabolism under nutrient limitation	760, 730, 40, 350, 272, 380, 450, 340
	Essential metabolic pathways	30, 920, 500
	Biosynthesis and degradation pathways	632, 626, 790

TABLE I. Microarray expression data shows that pathways associated with energy production, biosynthesis and metabolism peak at subjective dawn. The expression of house-keeping genes and pathways associated with DNA replication and repair peak at subjective dusk. Data reprinted from Vijayan *et al.* (supplemental information [1]).

SUPPLEMENTAL REFERENCES

[1] Vijayan, V., Zuzow, R. & O'Shea, E. K. Oscillations in supercoiling drive circadian gene expression in cyanobacteria. *Proceedings of the National Academy of Sciences* **106**, 22564–22568 (2009).